

Dear Dr. Li et al.

Based on two reviewers' comments on your article titled "Combined Impacts of ENSO and MJO on the 2015 Growing Season Drought over the Canadian Prairies", I am happy to say that final acceptance will take place, if you are able to address the reviewer's comments and suggestions - major revisions are required. Both reviewers have some excellent points and all of them can be reasonably addressed. I only point out some of the more major comments (and commonalities) below, however, each of the reviewer's points should be addressed as well.

We thank the editor and the two reviewers' valuable comments and advices to improve the original draft. Many improvements have been made to the draft according to the suggestion by the reviewers.

1) Both reviewers point out many typographical and grammatical errors. Please read over the manuscript carefully and make appropriate edits. One reviewer provided their marked-up manuscript to assist with this, as well as other comments requiring edits.

We have revised the draft accordingly to correct these errors.

2) Does the study period span 1979-2015 or 1979-2016?

The study period spans 1979-2016.

3) Manitoba is not included in the analysis. Hence, the title of the manuscript requires changing.

We acknowledge that the research only covers about the 2/3 of the agriculture land over the Prairies. We still hope to keep the title to "Combined Impacts of ENSO and MJO on the 2015 Growing Season Drought on Canadian Prairies" so that it is easier for researchers who are interested in the Prairies' precipitation to find the paper.

4) B.C. was not included in the analysis, but does appear to be affected. One reviewer is suggesting inclusion of B.C. or explaining why it was not included.

We choose to focus on the Prairie drought due to the fact the majority of the precipitation occur in summer for the Prairie whereas for BC coast the precipitation mainly occurs in winter. Though the precipitation deficit percent is high for BC coast. We have added some comments in the data section.

5) More quantitative analysis of the relation between Rossby waves and the drought should be addressed where possible.

We have added more analysis in terms of wave propagation.

6) Reviewer #2 suggests adding some detail about the unexplained drought events under NINO4>0 and MJO-4<0 (in the shaded region in Fig. 5), while connecting these events to the previously proposed teleconnection mechanisms in the introduction. At least some discussion should be made here.

We have added more discussions on the drought under NINO4>0 and MJO-4>0 and La Nina events.

7) The MJO-4 and ENSO are likely not independent. Some discussion of this should be made.

We have added discussions on the relationship between MJO and ENSO in the discussion section.

Once you have addresses each of the reviewer's comments, your manuscript will be considered for final publication.

Combined Impacts of ENSO and MJO on the 2015 Growing Season Drought on the Canadian Prairies

Zhenhua Li^{1,2}, Yanping Li¹, Barrie Bonsal³, Alan H. Manson², Lucia Sciff¹

¹Global Institute for Water Security, University of Saskatchewan, Saskatoon, Saskatchewan, Canada S7N3H5

²Institute of Space and Atmospheric Studies, University of Saskatchewan, Saskatoon, Saskatchewan, Canada

³National Hydrology Research Center, Environment and Climate Change Canada, Saskatoon, SK, Canada

Correspondence to: Dr. Yanping Li (yanping.li@usask.ca); Dr. Zhenhua Li (zhenhua.li@usask.ca)

Abstract

Warm-season precipitation on the Canadian Prairies plays a crucial role in agricultural production. This research investigates how the early summer 2015 drought across the Canadian Prairies is related to tropical Pacific forcing. The significant deficit of precipitation in May and June of 2015 coincided with a warm phase of El Niño-Southern Oscillation (ENSO) and a negative phase of Madden-Julian Oscillation (MJO)-4 index, which favour a positive geopotential height anomaly in western Canada. Our further investigation during the instrumental record (1979-2016) shows that warm-season precipitation in the Canadian Prairies and the corresponding atmospheric circulation anomalies over western Canada teleconnected with the lower boundary conditions in the tropical western Pacific. Our results indicate that MJO can play a crucial role in determining the summer precipitation anomaly in the western Canadian Prairies when the equatorial central Pacific is warmer than normal (NINO4 > 0) and MJO is more active. This teleconnection is due to the propagation of a stationary Rossby wave that is generated in the MJO-4 index region. When the tropical convection around MJO-4 index region (western tropical Pacific, centered over 140°E) is more active than normal (NINO4 > 0), a Rossby wave train originates from western Pacific and propagates into midlatitude over North America causing a persistent anomalous ridge in the upper level over western Canada, which favours dry conditions over the region.

1 Introduction

The Canadian Prairies depends on summer precipitation especially during the early to mid-growing season (May through August) when the majority of annual precipitation normally occurs (e.g.,

Deleted: over

Deleted: ,

Deleted: over

Deleted: activities in environment and society and has particular importance to

Deleted: over the region.

Deleted: a warm season precipitation deficit over

Deleted: in the early summer 2015 drought.

Deleted: were coincident

Deleted: as they both favor

Deleted: Further

Deleted: period

Deleted: 2015

Deleted: the

Deleted: .

Deleted: may

Deleted: Prairie

Deleted: The mechanism of this

Deleted: may be

Deleted: regions

Deleted:

Deleted: when

Deleted: .

Deleted: the

Deleted: an

Deleted: .

Deleted: are highly dependent

Deleted: July

53 Bonsal *et al.* 1993). High natural variability in growing season precipitation causes periodic occurrences
54 of extreme precipitation (Li *et al.* 2017, Liu *et al.* 2016 and droughts that are often associated with
55 reduced agriculture yields, low streamflow, and increased occurrence of forest fires (Wheaton *et al.*
56 2005, Bonsal and Regier 2007). Drought events with great environmental and economic impacts have
57 occurred in 1961, 1988, 2001-2002, and as recent as 2015 (Dey 1982, Liu *et al.* 2004, Bonsal *et al.*
58 1999, Wheaton *et al.* 2005, Shabbar *et al.* 2011, Bonsal *et al.* 2013, Szeto *et al.* 2016). The sub-seasonal

59 forecast of precipitation for the growing season is crucial for the agriculture, water resource
60 management, and the economy of the region. Therefore, an investigation into the causes of inter-annual
61 variability in the growing season precipitation of the Canadian Prairie is needed.

62 Low precipitation and extended dry periods on the Canadian Prairies are often associated with an
63 upper-level ridge and a persistent high pressure centered over the region (Dey 1982, Liu *et al.* 2004).

64 These prolonged atmospheric anomalies often concurred with abnormal boundary layer conditions such
65 as a large-scale sea surface temperature (SST) anomalies in the Pacific Ocean (Shabbar and Skinner
66 2004). Large scale oscillation in the SST anomalies in the Pacific Ocean, namely El Nino, and the
67 Pacific Decadal Oscillation (PDO), can affect the hydroclimatic pattern in summer over North America,
68 although the strongest impacts of these boundary conditions occur during the boreal winter. Inter-annual

69 variability such as El Nino-Southern Oscillation (ENSO) is linked with extended droughts in the Prairies
70 (Bonsal *et al.* 1999, Shabbar and Skinner 2004). Interdecadal oscillations such as the PDO, and the
71 Atlantic Multi-decadal Oscillation (AMO) also affect the seasonal temperature and precipitation in the
72 Canadian Prairies (Shabbar *et al.* 2011).

73 ENSO's relationship with Canadian Prairie precipitation has been studied extensively. The warm
74 phase of ENSO often favours drought in this region, especially during the growing season after the
75 mature phase of El Nino with the North Pacific Mode (NPM, Hartmann *et al.* 2015) positive like North
76 Pacific SST anomaly pattern (Bonsal and Lawford 1999, Shabbar and Skinner 2004). Previous

Deleted:)

Deleted: stream flow

Deleted: forecasting

Deleted: during

Deleted: are

Deleted: in

Deleted: potential

Deleted: the

Deleted: of

Deleted: much

Deleted: to provide important information for the agriculture and economy in the region.

Deleted: Prairies

Deleted: Decadal

Deleted:

Deleted: variabilities

Deleted: events are found to be

Deleted: oscillation

Deleted: have

Deleted: been found to

Deleted: the

Deleted: Prairies'

Deleted: the Canadian Prairies

Deleted:)

102 investigations (e.g., Shabbar *et al.* (2011)) have found [that](#) El Nino events are associated with a summer
103 moisture deficit in western Canada while La Nina events cause an abundance of moisture in [far](#) western
104 Canada (British Columbia and Yukon). However, they also noted that although tropical SST variability
105 accounted for some aspects of the large-scale circulation anomalies that influence Canadian Prairies
106 [meteorological](#) drought, a consistent and clear-cut relationship was not found. North Pacific SST warm
107 anomalies, which often follow a matured El Nino, and accompanying atmospheric ridging leads to
108 extended dry spells over the Prairies during the growing season (Bonsal and Lawford 1999).
109 [Furthermore, in association with](#) the recent North Pacific SST anomaly from 2013 to 2014, researchers
110 have attributed the precipitation deficit in California during 2013 to the anomalous upper-level ridge
111 over the western North America (Wang *et al.* 2014, Szeto *et al.* 2016).

Deleted: the

Deleted: extreme

Deleted: For

112 The [aforementioned](#) SST variations, mostly vary on [inter-annual](#) and decadal scales. Another
113 important factor that affects the weather patterns in North America is the Madden-Julian Oscillation
114 (MJO), an intra-seasonal (40-90 days) oscillation in convection and precipitation pattern [over](#) the
115 Tropics (Madden and Julian 1971, [Zhang 2005](#), Riddle *et al.* 2013, Carbone and Li 2015). MJO is a
116 coupled atmosphere-ocean oscillation involving [convection](#) and large-scale equatorial waves, which
117 produces an eastward [propagation](#) of tropical convection anomaly (Madden and Julian 1971). [The](#) MJO
118 [affects](#) the winter temperature and precipitation in North America and Europe through its impact on
119 moisture transport associated with [the](#) “Pineapple Express” and its effects on [the](#) North Atlantic
120 Oscillation and stratospheric polar vortex (Cassou 2008, Garfinkel *et al.* 2012, Rodney *et al.* 2013).
121 MJO [is also](#) connected to [the](#) summer precipitation [anomalies](#) in the Southwest United States (Lorenz
122 and Hartmann 2006). During [warm season](#), MJO's impact on Canadian [Prairie](#) precipitation has not been
123 thoroughly investigated as MJO's amplitude is weak during [spring and early](#) summer. The amplitude of
124 MJO in spring and early summer is related to the [inter-annual](#) variation of tropical SST, especially the
125 SST in central Pacific (Hendon *et al.* 2007, Marshall *et al.* 2016). MJO in terms of the Real-time

Deleted: formerly mentioned

Deleted: (ENSO, PDO, etc.)

Deleted: interannual

Deleted: in

Deleted: Zhang 2005,

Deleted: convections

Deleted: movement

Deleted: on an intraseasonal scale

Deleted: has been found to affect

Deleted: has been found to be

Deleted: precipitation anomalies to

Deleted: spring and summer

Deleted: the

Deleted: Prairies'

Deleted: , however,

Deleted: interannual

Deleted: The amplitude of

146 Multivariate MJO index (RMM, Wheeler and Hendon 2004) was extremely strong in the early spring of
147 2015 with a positive PDO-like SST anomaly in the central Pacific and at the same time, El Nino started
148 to strengthen.

Deleted:)

Deleted: high

Deleted: became strong

149 MJO activities in the western Pacific under the modulation of inter-annual SST variability have
150 the potential to act together with ENSO and impact mid-tropospheric circulation over western Canada
151 and thus, warm season precipitation over the Canadian Prairies. The goal of this study is to demonstrate
152 that MJO have contributed to the 2015 growing season drought in the Canadian Prairies through the
153 propagation of stationary Rossby wave. Subsequently, further investigations are carried out to determine
154 if similar relationships exist in association with other summer extreme precipitation events during

Deleted: interannual

Deleted: of SST

Deleted: the

Deleted: the mechanism involved

Deleted: may cause

Deleted: meteorological drought in

Deleted: in 2015

155 instrumental record (1979-2016). Section 2 provides the datasets and methodology used in this paper
156 while section 3 presents the analysis of the upper-level circulation anomaly and SST pattern associated
157 with the 2015 drought. This is followed by the examination of the effects of central Pacific SST
158 anomalies and MJO on the summer precipitation in the Canadian Prairies. The mechanism by which
159 MJO affects summer precipitation when equatorial central Pacific SST is warmer than normal is
160 discussed in section 4 followed by a summary and concluding remarks in section 5.

Deleted:

Deleted: methodologies

Deleted: analyses

Deleted:

Deleted:

Deleted: anomaly

Deleted: using data during instrumental record period.

Deleted: potential

Deleted: MJO affects

Deleted:

Deleted: of the results

161 2 Data and Methodology

162 Multiple observation and reanalysis datasets are used to investigate the circulation anomalies
163 associated with Canadian Prairie growing season (May-August) precipitation. Observed precipitation is
164 taken from the Climate Prediction Center (CPC) Merged Analysis of Precipitation (CMAP) dataset (Xie
165 and Arkin 1997). Geopotential height fields from the National Center for Environmental Predictions
166 (NCEP) Reanalysis (Kalnay et al. 1996) and the European Center for Medium-Range Weather Forecast
167 (ECMWF)'s ERA-Interim reanalysis (Dee et al. 2011) are used to analyze the mid- and upper-level (200
168 hPa and 500 hPa) atmospheric circulation patterns.

Deleted: 2.1 Data

Deleted: include those

Deleted: -interim

Deleted:), and

195 To represent the central Pacific SST anomaly, NINO4 SST index (Rayner *et al.* 2003) from CPC
 196 of National Oceanic and Atmospheric Administration (NOAA) is used since the NINO4 region is near
 197 [the](#) central Pacific and spans over the dateline (5°S-5°N, 160°E-150°W). Multivariate ENSO Index
 198 (MEI) data are retrieved from [NOAA's](#) Climate Data Center (CDC) website and [is](#) used to determine the
 199 ENSO phase (Wolter 1987, Wolter and Timlin 1993). In particular, El Nino condition is defined when
 200 the monthly mean index of MEI is larger than 0.5 (Andrews *et al.* 2004).

- Deleted: National Oceanic and Atmospheric Administration (NOAA)'s
- Deleted: are
- Deleted: an
- Deleted: as it identifies El Nino events consistently

201 The Real-time Multivariate MJO series (RMM1 and RMM2) developed by Wheeler and Hendon
 202 (2004) are used to [identify](#) periods of strong MJO [activity](#) as the MJO amplitudes are [directly calculated](#)
 203 by the square root of RMM1 + RMM2. For MJO intensities, we used the monthly averaged pentad MJO
 204 indices from NOAA CPC's MJO index (Xue *et al.* 2002) which have 10 indices representing locations
 205 around the globe. The CPC's MJO index is based on Extended Empirical Orthogonal Function (EEOF)
 206 analysis on pentad velocity potential at 200 hPa. Ten MJO indices [on a daily scale](#) are constructed by
 207 projecting the daily (00Z) velocity potential anomalies at 200 hPa (CHI200) onto the ten time-lagged
 208 patterns of the first EEOF of pentad CHI200 anomalies (Xue *et al.* 2002). Negative values of ten MJO
 209 indices correspond to enhanced [convection in the](#) 10 regions centered on 20°E, 70°E, 80°E, 100°E,
 210 120°E, 140°E, 160°E, 120°W, 40°W and 10°W in the tropics. MJO indices usually [vary](#) between -2 to 2,
 211 [with negative values indicating](#) above average convective activities in the corresponding region.

- Deleted: identified the
- Deleted: activities
- Deleted: readily available
- Deleted: calculation of the
- Deleted:
- Deleted: in a region
- Deleted:)
- Deleted: -
- Deleted: daily
- Deleted: -
- Deleted:
- Deleted: .
- Deleted: convections to
- Deleted: A negative value of the CPC's
- Deleted: (
- Deleted: varies
- Deleted:) indicates an

212 Because boreal summer [usually](#) corresponds to a period of weaker amplitude of MJO than [the](#) winter,
 213 we [chose the](#) monthly mean value of -0.3 as the criterion of strong [convection which is](#) connected to
 214 MJO, [as the index generally vary between -1 and 1. An MJO-4 index \(centered on 140°E\) of](#) less than -
 215 0.3 [was](#) considered a relatively strong convection in the western Pacific, [which](#) has been found to be a
 216 source region of stationary Rossby waves (Simmons 1980). SST observations include Extended
 217 Reconstructed Sea Surface Temperature (ERSST) v4 (Huang *et al.* 2015). Outward Longwave Radiation

- Deleted: choose
- Deleted: convections that are
- Deleted: . The monthly mean
- Deleted: is the criterion
- Deleted: as
- Deleted: associated with MJO
- Deleted: where
- Deleted:

248 (OLR) data from NOAA Interpolated Outgoing Longwave Radiation are used to derived the composite
 249 of anomalies of OLR for a certain phase of MJO.
 250 Our study focuses on growing season precipitation in the provinces of Alberta and Saskatchewan
 251 in the Canadian Prairies, where the largest deficits were observed in 2015. Specifically, the regional
 252 mean precipitation over 115°-102.5°W, 50°-57.5°N is used (boxed area in Fig. 1, top panel) to represent
 253 the Canadian Prairies east of the Rocky Mountains and south of the boreal forest. The region chosen
 254 also covers most of the arable land in the Canadian Prairies. Considering the unique MJO-4 and NINO4
 255 indices for 2015, the relationship between the Prairies' warm season (May-August) precipitation with
 256 MJO-4 and ENSO during the instrumental records are investigated using correlation and regression.

257 Though the dry months of the 2015 growing season are May and June when MJO-4 was in negative
 258 phase, we want to study the statistical relationship between MJO-4 and the Praries' precipitation in
 259 growing season (May-August). The possible mechanism behind the correlation between MJO-4 and the
 260 Prairie's warm season precipitation during El Nino condition is further investigated by analyzing the
 261 upper-level circulation associated with convection in the tropical Pacific and stationary Rossby waves in
 262 mid-latitudes.

264 3 Results

265 **3.1 The 2015 Summer Drought**

266 Almost all of western Canada including British Columbia, the southern Northwest Territories,
 267 Alberta and Saskatchewan had negative precipitation anomalies during May and June 2015. The top plot
 268 in Fig. 1 shows the precipitation anomaly in percentage relative to the climatology (1981-2010 long

Deleted: (hosted at
<http://www.esrl.noaa.gov/psd/map/clim/olr.shtml>)

Deleted: anomalous field

Deleted: as described below

Deleted: ¶

Moved down [1]: 3 Results¶

Deleted: This

Deleted: the

Deleted: arear

Deleted: Figure

Deleted: for datasets with 2.5-degree resolution. As

Deleted: indicated by the

Deleted: index

Deleted: investigation

Deleted: convections

Deleted: Tropics

Deleted: the midlatitudes

Deleted: ¶

Moved (insertion) [1]

Deleted: significant

Deleted: The warm season precipitation is represented by the monthly mean precipitation from May to August (Bonsal *et al.* 1999, Shabbar *et al.* 2011). For the 2015 case study, during May-June, the prairies' precipitation was significantly below average.

294 term mean) in Canada during May and June 2015. The bottom plot in Fig. 1 presents the monthly
 295 precipitation anomaly averaged over the region encompassed by the dash lines (top panel in Fig. 1). The
 296 average annual cycle of the regional precipitation has a dry period between February and May, and June
 297 has the largest precipitation in all months. The May and June 2015 precipitation deficit was also
 298 accompanied by a relatively dry period from February to April [Szeto *et al.* 2016], which added to the
 299 drought conditions.

300 Fig. 1 Top: Precipitation anomalies (mm) from CMAP over the region (115°W-102.5°W, 50°N-57.5°N) during May
 301 and June 2015. Bottom: time series of monthly precipitation anomaly over boxed region between September 2013 and
 302 August 2015.

303 The mid- and upper-level geopotential height (GHP) anomaly averaged in May and June are
 304 examined together with SST anomaly and ENSO, MJO-4 indices for 2014 and 2015. The 500 hPa GHP,
 305 anomaly for May and June 2015 shows strong positive anomalies near Alaska and the British Columbia
 306 coast (Fig. 2), which is consistent with the findings for other episodes of growing season droughts (e.g.,
 307 Dey 1982; Bonsal and Wheaton, 2005). Accompanying this anomalous ridge, are above normal SSTs in
 308 the northeast Pacific off the coast of North America and the central-eastern Pacific (Fig. 3). Both ENSO
 309 and the NPM are in positive phases that corresponds to a warmer SST near the Pacific coast of North
 310 America, consistent with the positive GPH anomalies in western Canada and Alaska. The ridge in
 311 Alaska/Bering Straits and the one near British Columbia coast have been previously associated with El
 312 Nino and North Pacific SST anomaly, such as NPM (Shabbar *et al.* 2011). The monthly mean anomalous
 313 ridge prevents storms from reaching the British Columbia coast and the Canadian Prairies causing
 314 extended dry spells. Therefore, the GPH anomaly in early growing season in 2015 is consistent with the
 315 precipitation anomaly in these regions. The anomalous upper-level ridge in the Western United States
 316 and Canada in 2014 and 2015 have also been associated with the developing El Nino and the other main

Deleted: 50N-57.5N, 115W-102.5W).

Deleted: , in average,

Deleted: Regarding the precipitation climatology, June

Deleted: with significantly more rain than neighboring months. When both

Deleted: witness much less

Deleted: than normal in addition to

Deleted: , the region gets little precipitation

Deleted:

Deleted:

Deleted:

Deleted:

Deleted: geopotential height (

Deleted:)

Deleted: the

Deleted: in

Deleted: ,

Deleted: extending from Alaska to Pacific Northwest of the US is an

Deleted: warm SST

Deleted: North Pacific Mode (NPM) (Hartmann *et al.* 2015)

Deleted: are

Deleted:

Deleted: indicates a tendency to prevent

Deleted: The

342 components of Pacific SST variation such as NPM by several recent studies (Hartmann *et al.* 2015, Lee
343 *et al.* 2015, Li *et al.* 2017).

344 Fig. 2 NCEP GPH anomaly at 500hPa during May and June 2015 when the precipitation deficit was the largest.

345 The average SST anomaly during the growing season (May-June, July-August) of 2015, shows a
346 persistent strong positive anomaly in the northeast and eastern equatorial Pacific (Fig. 3), which
347 corresponds to the warm phase of NPM and ENSO. SSTs in the eastern tropical Pacific warmed
348 increasingly since the end of 2014 and qualified as an El Nino in early 2015. The NPM became positive
349 in the fall 2013, turned exceptionally strong in 2014 and persisted to 2015 (Hartmann 2015). The
350 anomalous ridge is concurrent with strong SST anomalies in the tropical Pacific and extratropical North
351 Pacific. NPM, as the third EOF of Pacific SST (30°S-65°N), has also a strong connection to the
352 anomalous ridge in western North America and trough in the eastern US and Canada in 2013-2014
353 winter (Hartmann 2015, Lee *et al.* 2015). During the ENSO-neutral condition in 2013 and 2014, the
354 precursor of ENSO, so-called "footprinting" mechanism is considered to cause this anomalous ridge in
355 western North America (Wang *et al.* 2014).

356 The variation of Canadian Prairies' precipitation and its relationship with SST modes and MJOs
357 are shown in Fig. 4. The time series of monthly RMM amplitude, NINO4 index, MJO-4 indices and the
358 Canadian Prairies precipitation anomaly from January 2014 to December 2015 shows the atmospheric-
359 oceanic circulation indices for the drought in 2015. In May and June 2015, the western Pacific
360 witnessed a strong MJO-4 negative index, whereas in July the MJO-4 index became positive. This
361 corresponds well with the precipitation anomaly in Fig. 1. As shown in Fig. 3, El Nino continued to
362 strengthen in July and August 2015; while at the same time the MJO-4 index increased. The increase of
363 the MJO-4 index corresponded to the active convection associated with MJO that moved away from the

Deleted: sea surface temperature (
Deleted:)

Deleted: Fig. 3 shows the

Deleted: The

Deleted: Northeast Pacific

Deleted: is evident and persistent through the summer,

Deleted: , respectively. SST

Deleted: warms

Deleted: qualifies

Deleted: becomes

Deleted: since

Deleted: and turns to

Deleted: persist

Deleted: both

Deleted: 30S-65N),

Deleted: has

Deleted: the

Deleted: by some researchers

Deleted: the

Deleted: Summer of 2015 is the first summer after the developing El Nino during 2014-2015 winter. Though the upper-level GPH pattern seen in summer 2015 can be attributed to the SST modes in the Pacific Basin, namely ENSO and NPM, the precipitation in the Western Canadian Prairie is not strongly correlated with either of them. Bonsal and Lawford (1999) found that more extended dry spells tend to occur during the second summer following the mature stage of the El Nino events. The winter precipitation in Canada has been shown to have a strong connection to ENSO (Shabbar *et al.* 1997), whereas summer precipitations in most regions of western Canada (except the coast of British Columbia and Southern Alberta) do not have significant correlations with ENSO. This is consistent with [1]

Deleted: the

Deleted: anomaly

Deleted: condition

Deleted: 2015 both

Deleted: saw

Deleted: indices

Deleted: quite

Deleted: the 0EI

Deleted: in

Deleted: meantime,

Deleted: in July and August 2015.

Deleted: convections

Deleted: in West

426 [tropical western Pacific region and](#) propagated eastward into the central Pacific. [Coincident with this](#)
 427 [change in MJO](#), the precipitation in the Canadian [Prairies then](#) returned to slightly above normal in July.
 428 The good correspondence of MJO-4 and [the](#) negative precipitation anomaly suggests a link
 429 between MJO [and Prairie](#) precipitation during growing season. [Although](#) El Nino and associated
 430 Northeast Pacific [SST](#) warm anomaly (i.e., NPM) in summer 2015 can be a contributing factor for the
 431 [persistent](#) upper-level ridge [over](#) the west coast of Canada, it cannot fully explain the drought condition
 432 in [west](#) Canada, as these [SSTs do](#) not guarantee a prolonged dry spell as shown by correlation analysis,
 433 [\(Table 1\)](#). The negative MJO-4 index concurred with the negative anomaly of Prairie precipitation in
 434 2015, which prompts the investigation of their relationship [with](#) the instrumental records.

Deleted: ;

Deleted: Prairie

Deleted: index

Deleted: related tropical convection anomaly and the prairie

Deleted: Though

Deleted: on

Deleted: West

Deleted: SST conditions does

Deleted: .

Deleted: in

435 Fig. 3 The mean SST anomaly (°C) from ERSST v4 in May-August 2015.

436 Fig. 4 RMM amplitude anomaly, NINO4, MJO 4 indices and precipitation anomaly of Canadian Prairies from January 2014
 437 to Dec 2015.

438

439 3.2 Instrumental record

440 El Nino and its associated North Pacific SST anomaly may contribute to extended dry spells in
 441 Canadian Prairies after the [mature](#) phase of El Nino (Bonsal *et al.* 1993) on an [inter-annual](#) time scale.
 442 ENSO, however, is not a strong intra-seasonal to seasonal predictor of Canadian Prairie summer
 443 precipitation. [The lack of strong correlation between the Prairies' precipitation and ENSO index can be](#)
 444 [caused by many factors that affect the Prairies' precipitation on a seasonal and sub-seasonal scale.](#)
 445 [Shabbar and Skinner \(2004\) showed the connection between the warm phase of ENSO and western](#)
 446 [Canadian drought through singular value decomposition analysis. However, they also found other](#)
 447 [modes of SST variation \(e.g., positive phase of PDO\) can produce wet condition in the Prairies.](#) Here we
 448 present a new result showing that under warm central Pacific SST [conditions](#) (NINO4 >0), a certain

Deleted: matured

Deleted: interannual

Deleted: condition

462 phase of MJO, which connected to the active [convection](#) in the tropical western Pacific (Li and Carbone
 463 2012), plays an important role [in modulating](#) the [growing season](#) precipitation in the Canadian Prairies,
 464 Table 1 Correlation between mean precipitation anomaly [in the Prairies](#) from CMAP and MEI, MJO indices 4. MJO
 465 indices and [CMAP](#) are from 1979 to 2016.

- Deleted: convections
- Deleted: to determine
- Deleted: in the early summer months
- Deleted: in the prairie
- Deleted: CMAP covers 1979 to 2016. →

467 The correlation coefficients between the mean regional precipitation anomaly over Canadian
 468 Prairies and MJO-4 indices and MEI from May to August are shown in Table 1. The correlation
 469 between MEI [alone](#) and the precipitation anomalies is not significant. The correlation between MJO-4
 470 and precipitation in the Prairies [is 0.18 with a p-value of 0.023, which](#) indicates that stronger tropical
 471 [convection](#) in the [equatorial](#) region centered around 140°E [favours](#) less precipitation in the Canadian
 472 Prairies from May to August. [When NINO4 is larger than 0, the](#) correlation between MJO-4 and
 473 [growing season precipitation is](#) 0.33 with a p-value of 0.0015. [Conversely, the](#) correlation between
 474 MJO-4 and Canadian Prairie precipitation [is -0.01](#) when NINO4 < 0.

- Deleted: The negative MJO-4 index represents a stronger than normal convection in the Maritime Continents and the tropical Western Pacific.
- Deleted: index
- Deleted: convections
- Deleted: Equatorial
- Deleted: favor
- Deleted: The
- Deleted: index
- Deleted: the
- Deleted: Prairie

475 Fig. 5 The [scatter plot](#) of monthly precipitation anomaly (mm/month) as a function of MJO-4 and NINO4. Each
 476 asterisk represents a month from May to August 1979-2016. Circled asterisk denotes a month with precipitation anomaly larger
 477 than 18 mm/month. The blue circles are months with positive precipitation anomaly and the red circles are months with negative
 478 precipitation anomaly. The sizes of circles denote the magnitudes of the anomalies (large > 30 mm/month, medium > 24
 479 mm/month, small > 18 mm/month). The shaded area denotes NINO4 > 0 and MJO-4 index < 0.

- Deleted: anomaly is 0.18 with a p-value of 0.023. The correlation between MJO-4 index and the precipitation anomaly during growing season when NINO4 > 0 is much higher at
- Deleted: The
- Deleted: the
- Deleted: is -0.01
- Deleted: scatterplot
- Deleted:
- Deleted:
- Deleted: >
- Deleted: , which together affect the precipitation anomaly from May to August.
- Deleted: .
- Deleted: sizes

480 The scatter plot in Fig. 5 shows the distribution of monthly precipitation anomaly versus MJO-4
 481 index and NINO4 index. Circled asterisk denotes a month with precipitation anomaly larger than 18
 482 mm/month and the red (blue) circles denote a negative (positive) precipitation [anomaly](#). The [criterion](#)
 483 [for precipitation anomaly to be emphasized by the circles is roughly one third of the mean monthly](#)
 484 [precipitation in the growing season. The size](#) of the circle [represents](#) the magnitude of the monthly
 485 precipitation anomalies. [The](#) bottom-right region indicated by shading, under NINO4 > 0 condition,

- Deleted: represent
- Deleted: In the

519 negative MJO-4 corresponds to a quadrant that have many more dry than wet months. We noticed that
 520 some significant dry months are not in the shaded area, which corresponds to the dry months occurring
 521 during La Nina or in the period after the mature phase of El Nino (Bonsal *et al.* 1999). Summer drought
 522 in the Prairies can occur in both phases of ENSO or any other teleconnection indices. For example, for
 523 the summer drought that happened in the Prairies from 1999 to 2005, the large-scale anomalous patterns
 524 of SST first showed La Nina conditions and then became a weak El Nino in the latter half of the period
 525 (Hanesiak *et al.* 2011). Bonsal and Wheaton (2005) showed that the tropospheric atmospheric
 526 circulation patterns in 2001 and 2002 lacked the typical meridional flow in the North Pacific and North
 527 America during drought in western Canada. Their results show that the drought in 1999-2005 was
 528 related to the expansion of the continuous drought happened in the US to the north.

Deleted: months

Deleted: region

Deleted: occur in

Deleted: condition

529 Fig. 6 The box-percentile plot of Canadian Prairies precipitation anomaly during growing season under different
 530 ENSO conditions.

Deleted: for

531 The impact of ENSO on the growing season precipitation over Canadian Prairies is investigated.
 532 The box-percentile plot in Fig. 6 shows the distribution of monthly Canadian Prairies' precipitation
 533 anomalies from May to August along with different ENSO conditions. In general, under El Nino and
 534 neutral ENSO conditions, the precipitation anomalies are centered around 0, and there is no bias toward
 535 either end. Under La Nina condition, the mean precipitation has a positive bias. There are only 10
 536 summer months under La Nina condition, whereas there are 71 months under El Nino and neutral
 537 condition.

Deleted: To investigate the

Deleted: , the distribution of precipitation anomaly along ENSO conditions are plotted

Deleted: condition

Deleted: ENSO

Deleted: condition

Deleted: on

Deleted:

Deleted: both

Deleted: have 71 months

Deleted: Under warm central Pacific SST condition (

Deleted:),

Deleted: for

Deleted: Under

Deleted: >

Deleted: condition

Deleted: such

Deleted: the precipitation anomaly under the condition of

Deleted: Based on

Deleted: ,

Deleted: condition

Deleted: is demonstrated in detail.

538 The distributions of precipitation anomalies versus MJO-4 index under different ENSO
 539 conditions are shown in Fig. 7. For NINO4 > 0, the precipitation anomaly has a negative tendency when
 540 MJO-4 < -0.3. With NINO4 ≤ 0, there is no negative tendency for MJO-4 < -0.3. Therefore, Fig. 6 and 7
 541 agrees with the significant correlation between precipitation and MJO-4 under NINO4 > 0, relative to
 542 ENSO in Table 1.

570 Fig. 7 Box-percentile plots of Canadian Prairies' precipitation anomaly during growing season versus MJO-4 under
571 warm NINO4 (NINO4 > 0, left) and cold NINO4 (NINO4 < 0, right) SST condition.

572 The correlation between MJO-4 and the Prairies' precipitation during growing season leads us to
573 investigate the underlying circulation anomalies. Fig. 8 presents the regressed stream function and wind

574 field at 200 hPa in the mid-latitudes (north of 30°N) on the negative MJO-4 index from May to August

575 under warm NINO4 SST condition (NINO4 > 0.5). In the tropics (10°S-20°N), during Northern

576 Hemisphere summer, the OLR, velocity potential, and divergent wind vector are presented. Only

577 regression patterns having p-values lower than 0.05 are plotted for OLR and velocity potential. The

578 negative MJO-4 index corresponds to a negative anomaly in OLR, stronger convection and larger than

579 average divergence in the region centered around 150°E. The strong convection anomaly centers around

580 150°E, 5°N with divergent wind extending well into the subtropics in the Northern Hemisphere. The

581 positive GPH/stream function anomaly extended from Japan to central Pacific is associated with the

582 enhanced convection and divergence in the upper troposphere over the western tropical-subtropical

583 Pacific. A Rossby wave train linked to the OLR anomaly and strong divergence in the western Pacific

584 propagate eastward into North America. [To better demonstrate the propagation of the wave train, we](#)

585 [conducted a ray tracing of stationary Rossby wave following the nondivergent barotropic Rossby wave](#)

586 [theory of Hoskins and Karoly \(1981\) and Hoskins and Ambrizzi \(1993\). Equation 1 describes the group](#)

587 [velocity, which represent the propagation of wave activity.](#) C_{gx} and C_{gy} are the group velocity

588 [components on zonal and meridional directions;](#) \bar{U} and \bar{V} are the mean zonal and meridional winds; q is

589 [the mean absolute vorticity; \$K\$, \$k\$, \$l\$ are the total wave number, zonal wavenumber and meridional](#)

590 [wavenumber, respectively. The ray path is integrated using a fourth-order Runge-Kutta method.](#)

Deleted:

Deleted:

Deleted: strong

Deleted: prairie

Deleted: midlatitudes

Deleted: 30N

Deleted: >

Deleted: 10S-20N, considering it is

Deleted:),

Deleted: ,

Deleted: plotted

Deleted: have

Deleted: on

Deleted:

Deleted: on

Deleted:

Deleted:

$$C_{gx} = \bar{U} + \frac{(k^2 - l^2)q_y - 2klq_x}{K^4}$$

Equation (1)

$$C_{gy} = \bar{V} + \frac{(k^2 - l^2)q_x + 2klq_y}{K^4}$$

Under average conditions in May-August derived from ERA-Interim at 200 hPa with NINO4 > 0.5 or NINO4 < -0.5, we released rays with a total wavenumber matching with the mean flow at the extratropical location of the OLR anomaly (140°E-150°E, 25°N-30°N). For quasi-stationary waves, the wavenumber is determined by the basic zonal flow and background absolute vorticity gradient through the dispersion relation. For NINO4 > 0.5 May-August condition, K = 4.14. With this total wavenumber and launching angle from 0- 60° relative to the zonal direction, Rossby wave rays (colored by red, orange to blue according to their angle from 0° to 60°) released at 140°W, 20°N can propagate successfully to the western Canada for those with smaller launching angles as shown the right in Fig. 9. With NINO4 < -0.5, the zonal wind in the source region is weaker, and the meridional gradient of absolute vorticity is stronger due to its relative further southern position to the subtropical jet. The total wavenumber for stationary Rossby waves is 6.2, determined by the mean May-August condition for NINO4 < -0.5. The waves with shorter wavelength tend to be evanescent near the source region as shown in the left plot in Fig. 9. However, there is no significant difference in ray-path under NINO4 < -0.5 condition compared to NINO4 > 0.5, if the source wavenumbers are set to the same value (results not shown). The changes in the mean conditions from El Nino to La Nina are not sufficient to alter the propagation condition for Rossby waves.

4 Discussion

Summer of 2015 is the first summer after the developing of El Nino during 2014-2015 winter. Though the upper-level GPH pattern, seen in summer 2015, can be attributed to the SST modes in the Pacific, namely ENSO and NPM, the precipitation in the Western Canadian Prairie is not strongly correlated with either. Bonsal and Lawford (1999) found that more extended dry spells tend to occur in Canadian Prairies during the second summer following the mature stage of the El Nino events. The winter precipitation in Canada has a strong connection to ENSO (Shabbar *et al.* 1997), whereas summer precipitation, in most regions of western Canada (except the coast of British Columbia and Southern Alberta), does not have a significant correlation with ENSO. This is consistent with our investigation using instrumental records from 1948 to 2016.

Growing season precipitation in the Canadian Prairies is affected by many factors, precipitation deficits can occur under various circulation and lower boundary conditions. Thus, it is not expected that a universal condition for all the significant droughts in the region can be identified. In fact, extreme drought events have been found in both El Nino and La Nina years. A previous study by Bonsal and Lawford (1999) indicates the meteorological drought often occurs after the mature phase of El Nino, which is not the case for 2015. The associated changes in the North Pacific represented by NPM positive phase is consistent with their results. The direct linkage between ENSO and the summer precipitation in the Canadian Prairies is not clear. In fact, the correlation between MEI and precipitation in the investigated region is -0.096 ($p=0.239$, sample size = 152). The region's growing season precipitation does not possess a significant correlation with ENSO, which is consistent with other researchers' findings (Dai and Wigley 2000).

The regression pattern is consistent with stationary Rossby wave theory as shown in a hierarchy of theoretical and modeling studies (Karoly *et al.* 1989, Simmons *et al.* 1983, Hoskins and Ambrizzi

Moved (insertion) [2]

Deleted: growing

Deleted: are

Deleted: and

Deleted: deficit

Deleted: to find

Deleted: .

Deleted: conditions

Deleted: and La Nina years. Though

Deleted: research

Deleted: , the

Deleted: still

Deleted: 2389

Deleted: It is

666 1993, Ambrizzi and Hoskins 1997, Held *et al.* 2002). A similar wave train extends from the western
 667 Pacific toward [extra-tropical](#) South America but at lower latitudes compared to its counterpart in the
 668 Northern Hemisphere (not shown). The node of the wave train in Western Canada and Northwest
 669 Pacific of the US corresponds to an anomalous ridge, which is in-phase of El Nino forcing. When the
 670 convection in the region associated with MJO-4 is weaker than normal (MJO-4 ≤ 0), a wave train with
 671 the opposite sign [will](#) reach western Canada which [then counteracts the](#) El Nino forcing. Thus, the weak
 672 correlation between Canadian Prairie precipitation and ENSO is understandable as MJO plays an
 673 additional role that enhances or cancels out the GPH anomaly caused by El Nino.

674 [In mid-latitude North America, the](#) atmospheric response to the tropical forcing in the western
 675 Pacific depends on the mean circulation condition associated with tropical SST. Intraseasonal tropical
 676 convection oscillation in the western Pacific associated with MJO-4 index cannot determine the sign of
 677 precipitation anomaly in the [prairies alone](#). Both warm SST in central Pacific and strong tropical
 678 convection in western Pacific and Maritime Continent are [essential](#) to cause a significant precipitation
 679 deficit in the western Canadian Prairies. Warm SST in central Pacific causes an eastward expansion of
 680 Pacific warm pool that [favours](#) enhanced MJO activity in the western-central Pacific (Hendon *et al.*
 681 1999, Marshall *et al.* 2016). [In the year 2015, the SST anomaly in the Pacific \(e.g. ENSO, NPM\) forced](#)
 682 the anomalous ridge on the west coast of Canada. [This positive GPH anomaly was associated with the](#)
 683 [strong negative MJO4 indices, it then caused a blocking pattern and suppressed](#) precipitation in the
 684 Canadian Prairies in the early summer. Although the El Nino continued to strengthen in July and August
 685 2015, the active [convection](#) associated with MJO in [the western](#) Pacific propagated eastward into the
 686 central Pacific. [As](#) the convection in the western Pacific/Maritime Continent waned, the precipitation in
 687 the Canadian Prairie returned to slightly above normal in July.

Deleted: in the extratropics

Deleted: >

Deleted: would

Deleted: would counteract on

Deleted: The

Deleted: in midlatitude North America

Deleted: prairie.

Deleted: necessary

Deleted: favors

Deleted: For

Deleted: of

Deleted: while the anomalous positive GPH associated with strong negative MJO4 indices in addition to

Deleted: which reduces

Deleted: convections

Deleted: West

Deleted: , as

705 Fig. 8 The regression of stream function, wind field in the extratropics on MJO-4 for May-August with MEI ≥ 0.5 .
 706 Bottom: OLR, velocity potential, and divergent wind in the tropics on MJO-4 indices for May-August with
 707 $NINO4 > 0.5$. The shaded region for the tropical OLR has p-value ≤ 0.05 . Blue shading indicates active convection region.
 708 Red dashed contour and solid blue contour corresponds to negative and positive velocity potential, respectively.

Deleted: >

Deleted: $NINO4 > 0$.

Deleted: <

710 5 Conclusions

711 The cause of the 2015 summer precipitation deficit in the western Canadian Prairies is
 712 investigated in relation to atmospheric circulation anomalies, SST, and intraseasonal tropical convection
 713 oscillation, MJO. The drought in western Canada is immediately related to an anomalous upper-level
 714 ridge that persisted over the west coast of Canada and Alaska since fall 2014. This ridge was likely
 715 associated with a developing El Nino that was enhanced by the MJO.

Deleted: regarding

Deleted: sea surface temperature

Deleted: the

Deleted: ridge in the

Deleted: The persistent anomalous upper-level ridge hovering around

Deleted: is

Deleted: SST anomaly in the tropical (ENSO) and extratropical Pacific (NPM) as both SST patterns tend to associate with an anomalous high in Alaska and western Canada. However, the anomalous ridge itself explains the drought in the western Canada, the underlying cause of the anomalous ridge and whether it is related to ENSO need investigation. After all the significant deficit of precipitation concentrated in May and June 2015 when

716 In general, MJO-4 indices demonstrated significant correlation with the meteorological drought
 717 happened over west Canadian Prairies from May to August when warm SST presented in central Pacific
 718 ($NINO4 > 0$) with strong MJO amplitude. Our study discovered that MJO phase/strength is connected to
 719 the anomalous ridge over western Canada through the propagation of stationary Rossby wave from the
 720 western Pacific when NINO4 is positive. Though seasonally MJO is weaker in summer, the spring and
 721 early summer MJO amplitude is larger than normal when the central Pacific SST is warmer than normal
 722 ($NINO4 > 0$). The teleconnection between the Canadian Prairie precipitation deficit and MJO is stronger
 723 when NINO4 is positive. The underlying cause of this significant correlation between MJO-4 indices
 724 and the prairie precipitation in May-August is a stationary Rossby wave train originating from the
 725 Maritime Continent and western Pacific which propagates into Canada. The raytracing experiments
 726 show the main difference between a warm phase of NINO4 and a cold phase is the changes in stationary
 727 Rossby wave wavenumber over the source region. Under NINO4 > 0.5 May-August condition, the total

Deleted: was still growing in intensity. The correlation of ENSO with the prairie precipitation is also not significant during summer. Instead, the intraseasonal oscillation in tropical convection,

Deleted: , plays an important role in determining precipitation anomaly during months with warm central Pacific SST ($NINO4 > 0$).

Deleted: demonstrate

Deleted: with

Deleted: when

Deleted: is also often stronger. The new finding in our investigation is

Deleted: in Western

Deleted: when NINO4 is positive

Deleted: . The connection

Deleted: because MJO amplitude is stronger when the central Pacific SST is warmer than normal ($NINO4 > 0$).

Deleted: originates

Deleted: and

765 [wavenumber is about 4 and can propagate into western Canada if they oriented relatively zonally.](#)
766 [Compared to NINO4 > 0.5, NINO4 < -0.5 corresponds to a weaker zonal wind and stronger meridional](#)
767 [gradient of absolute vorticity in the subtropics of the source region \(140-150E\), hence the wavenumbers](#)
768 [of stationary Rossby waves from the source region are larger \(about 6\), and fail to reach the Western](#)
769 [Hemisphere.](#) The intra-seasonal predictability of the growing season precipitation in the Canadian
770 Prairies [can be potentially improved by including the MJO amplitude and phase factors for medium-](#)
771 [range/intra-seasonal projection in addition to ENSO effect especially](#) when the central-Pacific SST is
772 warm.

Deleted: Canada.

Deleted: in MJO amplitude and phase can be potentially instrumental for medium-range/intra-seasonal projection

774 Acknowledgement

775 We gratefully acknowledge the Natural Sciences and Engineering Research Council of Canada
776 (NSERC) for funding the Changing Cold Regions Network (CCRN) through their Climate Change and
777 Atmospheric Research (CCAR) Initiative. Dr. Zhenhua Li is supported by the Probing the Atmosphere
778 of the High Arctic project sponsored by the NSERC. [Dr. Yanping Li gratefully acknowledges the](#)
779 [support from the Global Institute of Water Security at the University of Saskatchewan. This research is](#)
780 [also supported by Environment and Climate Change Canada \(ECCC\).](#)

Moved down [4]: This research is also supported by Environment and Climate Change Canada (ECCC). Dr.

Moved up [3]: Dr.

Moved (insertion) [3]

Deleted: Y.

Moved (insertion) [4]

781 References

782 Ambrizzi T and Hoskins B J 1997: Stationary Rossby-Wave Propagation in a Baroclinic Atmosphere,
783 *Quart. J. Roy. Meteor. Soc.*, **123** 919–28.
784 Andrews, E.D., R.C. Antweiler, P.J. Neiman, and F.M. Ralph 2004 Influence of ENSO on Flood
785 Frequency along the California Coast. *J. Climate*, **17**, 337–348, doi: 10.1175/1520-0442(2004)017.

793 Bonsal, B.R., Chakravarti, A.K. and Lawford, R.G. 1993: Teleconnections between North Pacific SST
794 Anomalies and Growing Season Extended Dry Spells on the Canadian Prairies, *Int. J. Climatol.*, 13,
795 865-878.

796 Bonsal, B.R., Zhang, X. and Hogg, W.D., 1999: Canadian Prairie growing season precipitation
797 variability and associated atmospheric circulation, *Climate Research*, 11(3), 191-208.

798 Bonsal B and Lawford R 1999: Teleconnections between El Niño and La Niña Events and Summer
799 Extended Dry Spells on the Canadian Prairies, *International Journal of Climatology*, 19, 1445–58.

800 Bonsal B R, Shabbar A and Higuchi K, 2001: Impacts of Low Frequency Variability Modes on
801 Canadian Winter Temperature, *Int. J. Climatol.* 21, 95–108.

802 [BONSAL, B.R. and E. WHEATON. 2005: Atmospheric circulation comparisons between the 2001](#)
803 [and 2002 and the 1961 and 1988 Canadian Prairie droughts. *Atmosphere-Ocean*, 43 \(2\): 163–](#)
804 [172.](#)

805 Bonsal B R and Regier M, 2007: Historical Comparison of the 2001/2002 Drought in the Canadian
806 Prairies, *Climate Research*, 33, 229-242.

807 Bonsal, B R, Aider, R, Gachon, P and Lapp S, 2013: An Assessment of Canadian Prairie Drought: Past,
808 Present, and Future, *Climate Dynamics*, 41, 501–516.

809 Carbone R. E., Yanping Li, 2015: Tropical Oceanic Rainfall and Sea Surface Temperature Structure:
810 Parsing Causation from Correlation in the MJO, *Journal of Atmospheric Science*, Vol. 72, No. 7, 2703–
811 2718.

812 Cassou C, 2008: Intraseasonal Interaction Between the Madden-Julian Oscillation and the North
813 Atlantic Oscillation, *Nature*, 455 523–7.

814 Dai A and Wigley T M L, 2000: Global Patterns of ENSO-Induced Precipitation, *Geophys. Res. Lett.*,
815 27 1283–6.

816 Dee D P, Uppala S M, Simmons A J, Berrisford P, Poli P, Kobayashi S, Andrae U, Balmaseda M A,
817 Balsamo G, Bauer P, Bechtold P, Beljaars A C M, Berg L van de, Bidlot J, Bormann N, Delsol C,
818 Dragani R, Fuentes M, Geer A J, Haimberger L, Healy S B, Hersbach H, Hólm E V, Isaksen L, Kållberg
819 P, Köhler M, Matricardi M, McNally A P, Monge-Sanz B M, Morcrette J-J, Park B-K, Peubey C,
820 Rosnay P de, Tavolato C, Thépaut J-N, and Vitart F, 2011: The ERA-Interim Reanalysis: Configuration
821 and Performance of the Data Assimilation System, *Quarterly Journal of the Royal Meteorological*
822 *Society*, **137**, 553–97.

823 Dey B, 1982: Nature and Possible Causes of Droughts on the Canadian Prairies-Case Studies, *Journal of*
824 *Climatology*, **2**, 233–49.

825 Garfinkel C I, Feldstein S B, Waugh D W, Yoo C and Lee S, 2012: Observed Connection Between
826 Stratospheric Sudden Warmings and the Madden-Julian Oscillation, *Geophys. Res. Lett.*, **39**.

827 [Hanesiak, J. M., Stewart, R. E., Bonsal, B. R., Harder, P., Lawford, R., Aider, R., et al. \(2011\).](#)
828 [Characterization and Summary of the 1999–2005 Canadian Prairie Drought. *Atmosphere-Ocean*, 49\(4\),](#)
829 [421–452. <http://doi.org/10.1080/07055900.2011.626757>](#)

830 Hartmann D L, 2015: Pacific Sea Surface Temperature and the Winter of 2014, *Geophys. Res. Lett.*, **42**,
831 1894–902.

832 Held I. M., Ting M. and Wang H., 2002: Northern Winter Stationary Waves: Theory and Modeling *J.*
833 *Climate*, **15**, 2125–44.

834 Hendon, H. H., C. Zhang, and J. D. Glick, 1999: Interannual variation of the Madden-Julian Oscillation
835 during Austral summer, *J. Clim.*, **12**, 2538–2550

836 Hong, C. C., Hsu, H. H., Tseng, W.-L., Lee, M. Y., Chow, C.-H., & Jiang, L.-C. 2017: Extratropical
837 Forcing Triggered the 2015 Madden–Julian Oscillation–El Niño Event. *Sci. Rep.* **7**, 46692; doi:
838 10.1038/srep46692.Hoskins B J and Ambrizzi T, 1993: Rossby Wave Propagation on a Realistic
839 Longitudinally Varying Flow. *J. Atmos. Sci.* **50** 1661–71

840 [Hoskins, B.J. and D.J. Karoly, 1981: The Steady Linear Response of a Spherical Atmosphere to](#)
841 [Thermal and Orographic Forcing. *J. Atmos. Sci.*, **38**, 1179–1196, \[https://doi.org/10.1175/1520-\]\(https://doi.org/10.1175/1520-0469\(1981\)038<1179:TSLROA>2.0.CO;2\)](#)
842 [0469\(1981\)038<1179:TSLROA>2.0.CO;2](#)

843 [Hoskins, B.J. and T. Ambrizzi, 1993: Rossby Wave Propagation on a Realistic Longitudinally Varying](#)
844 [Flow. *J. Atmos. Sci.*, **50**, 1661–1671, \[https://doi.org/10.1175/1520-\]\(https://doi.org/10.1175/1520-0469\(1993\)050<1661:RWPOAR>2.0.CO;2\)](#)
845 [0469\(1993\)050<1661:RWPOAR>2.0.CO;2](#)

846 Huang B, Banzon V F, Freeman E, Lawrimore J, Liu W, Peterson T C, Smith T M, Thorne P W,
847 Woodruff S D and Zhang H-M, 2015: Extended Reconstructed Sea Surface Temperature Version 4
848 (ERSST. v4). Part I: Upgrades and Intercomparisons *Journal of Climate*, **28**, 911–30.

849 Kalnay E, Kanamitsu M, Kistler R, Collins W, Deaven D, Gandin L, Iredell M, Saha S, White G,
850 Woollen J, Zhu Y, Chelliah M, Ebisuzaki W, Higgins W, Janowiak J, Mo K, Ropelewski C, Wang J,
851 Leetmaa A, Reynolds R, Jenne R and Joseph D, 1996: The NCEP/NCAR 40-Year Reanalysis Project
852 *Bull. Amer. Meteor. Soc.* **77** 437–71

853 Karoly D J, Plumb R A, and Ting M, 1989: Examples of the Horizontal Propagation of Quasi-Stationary
854 Waves. *J. Atmos. Sci.* **46** 2802–11

855 Lee M Y, Hong C C and Hsu H H 2015: Compounding Effects of Warm Sea Surface Temperature and
856 Reduced Sea Ice on the Extreme Circulation Over the Extratropical North Pacific and North America
857 During the 2013/2014 Boreal winter *Geophys. Res. Lett.*, **42**, 1612–8.

858 [Li, Y., Richard E. Carbone, 2012: Excitation of rainfall over the tropical western Pacific. *Journal of*](#)
859 [Atmospheric Science](#), Vol. 69, No. 10, 2983–2994.

860 [Li, Y., Kit Szeto, Ron Stewart, Julie Theriault, Liang Chen, Bob Kochtubajda, Anthony Liu, Sudesh](#)
861 [Boodoo, Ron Goodson, Curtis Mooney, Sopan Kurkute, 2017: The June 2013 Alberta Catastrophic](#)

Deleted: Yanping

Deleted: ,

Deleted: Yanping

Deleted: ,

866 Flooding: Water vapor transport analysis by WRF simulation. *Journal of Hydrometeorology*, Vol. 18,
867 2057-2078.

868 [Li Z.](#), Alan Manson, Yanping Li, Chris Meek, 2017: Circulation Characteristics of Persistent Cold
869 Spells in Central-Eastern North America. *Journal of Met. Res.*, Vol. 31, 250-260.

870 Liu J, Stewart R E and Szeto K K, 2004: Moisture Transport and Other Hydrometeorological Features
871 Associated With the Severe 2000/01 Drought Over the Western and Central Canadian Prairies *Journal*
872 *Of Climate*, **17**, 305–19.

873 [Liu A., C. Mooney, K. Szeto, J. M. Thériault, B. Kochtubajda, R.E. Stewart, S. Boodoo, R. Goodson, Y.](#)
874 [Li, J. Pomeroy, 2016: The June 2013 Alberta Catastrophic Flooding Event: Part 1 – Large scale features.](#)
875 [Hydrological Process, 2016, 30, 4899–4916](#)

876 Lorenz, D.J. and D.L. Hartmann, 2006: The Effect of the MJO on the North American Monsoon. *J.*
877 *Climate*, **19**, 333–343, doi: 10.1175/JCLI3684.1.

878 Madden R A and Julian P R, 1971: Detection of a 40-50 Day Oscillation in the Zonal Wind in the
879 Tropical Pacific, *J. Atmos. Sci.*, **28**, 702–8

880 Marshall, A. G., H. H. Hendon, and G. Wang, 2016: On the role of anomalous ocean surface
881 temperatures for promoting the record Madden-Julian Oscillation in March 2015, *Geophys. Res. Lett.*,
882 43,472–481.

883 Riddle E E, Stoner M B, Johnson N C, L'Heureux M L, Collins D C and Feldstein S B, 2013: The
884 Impact of the MJO on Clusters of Wintertime Circulation Anomalies Over the North American region
885 *Climate Dynamics*, **40**, 1749–66.

886 Rodney, M., Lin, H., & Derome, J. 2013: Subseasonal Prediction of Wintertime North American
887 Surface Air Temperature during Strong MJO Events. *Monthly Weather Review*, *141*(8), 2897–2909.
888 <http://doi.org/10.1175/MWR-D-12-00221.1>.

Deleted: Zhenhua
Deleted: .

891 Ropelewski C F and Halpert M S 1986: North American Precipitation and Temperature Patterns
892 Associated with the El Niño/Southern Oscillation (ENSO), *Monthly Weather Review*, **114**, 2352–62.

893 Shabbar, A., Bonsal, B. and Khandekar, M., 1997: Canadian precipitation patterns associated with the
894 Southern Oscillation. *Journal of Climate* 10:3016-3027.

895 Shabbar A and Skinner W, 2004: Summer Drought Patterns in Canada and the Relationship to Global
896 Sea Surface Temperatures, *Journal of Climate*, **17**, 2866–80.

897 Shabbar A, Bonsal B R and Szeto K, 2011: Atmospheric and Oceanic Variability Associated with
898 Growing Season Droughts and Pluvials on the Canadian Prairies, *Atmosphere-Ocean*, **49**, 339–55.

899 Simmons A J, Wallace J M and Branstator G W, 1983: Barotropic Wave Propagation and Instability,
900 and Atmospheric Teleconnection Patterns, *J. Atmos. Sci.*, **40**, 1363–92.

901 Szeto, K., X. Zhang, R.E. White, and J. Brimelow, 2016: The 2015 Extreme Drought in Western
902 Canada. *Bull. Amer. Meteor. Soc.*, **97**, S42–S46, <https://doi.org/10.1175/BAMS-D-16-0147.1>.

903 Wang S Y, Hippias L, Gillies R R and Yoon J-H, 2014: Probable Causes of the Abnormal Ridge
904 Accompanying the 2013-2014, California Drought: ENSO Precursor and Anthropogenic Warming
905 footprint *Geophys. Res. Lett.*, **41** 3220–6.

906 Xie P and Arkin P A, 1997: Global Precipitation: A 17-year Monthly Analysis Based on Gauge
907 Observations, Satellite Estimates, and Numerical Model Outputs. *Bulletin of the American
908 Meteorological Society*, **78**, 2539–58.

909 Xue Y, Higgins W and Kousky V 2002: Influences of the Madden-Julian Oscillations on Temperature
910 and Precipitation in North America during ENSO-neutral and Weak ENSO Winters, *Proc. workshop on
911 prospects for improved forecasts of weather and short-term climate variability on subseasonal (2 week
912 to 2 month) time scales.*

913 Wheaton, E, Wittrock V, Kulshreshtha S, Koshida G, Grant C, Chipanshi A, Bonsal BR, 2005: Lessons
914 Learned from the Drought Years of 2001 and 2002: Synthesis Report. Agriculture and Agri-Food
915 Canada, Saskatchewan Research Council Publ No. 11602-46E03, Saskatoon.

916 Wheeler, M. C., & Hendon, H. H., 2004: An all-season real-time multivariate MJO index: Development
917 of an index for monitoring and prediction. *Monthly Weather Review*, 132(8), 1917-1932.

918 Wolter, K., 1987: The Southern Oscillation in surface circulation and climate over the tropical
919 Atlantic, Eastern Pacific, and Indian Oceans as captured by cluster analysis. *J. Climate Appl.*
920 *Meteor.*, 26, 540-558.

921 Wolter, K. and M.S. Timlin, 1993: Monitoring ENSO in COADS with a seasonally adjusted principal
922 component index. Proc. of the 17th Climate Diagnostics Workshop, Norman, OK,
923 NOAA/NMC/CAC, NSSL, Oklahoma Clim. Survey, CIMMS and the School of Meteor., Univ. of
924 Oklahoma, 52-57.

925 Zhang C, 2005: Madden-Julian Oscillation *Reviews of Geophysics*, 43.

926
927

Deleted: ↵



937

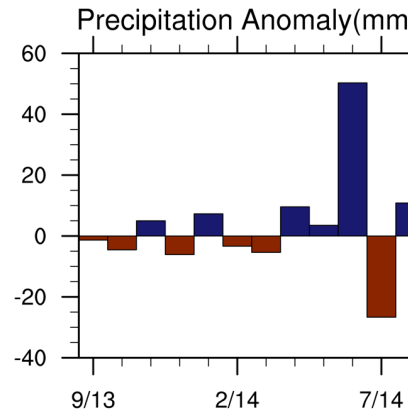
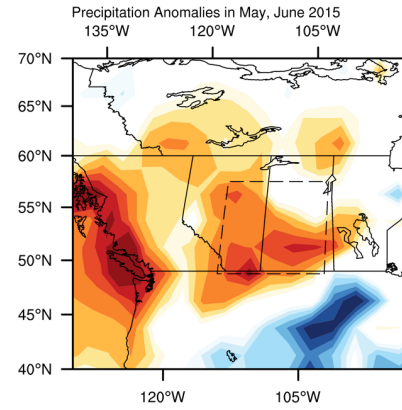
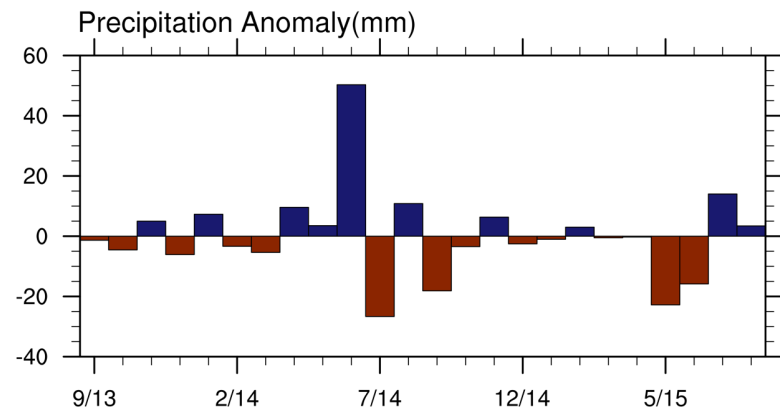
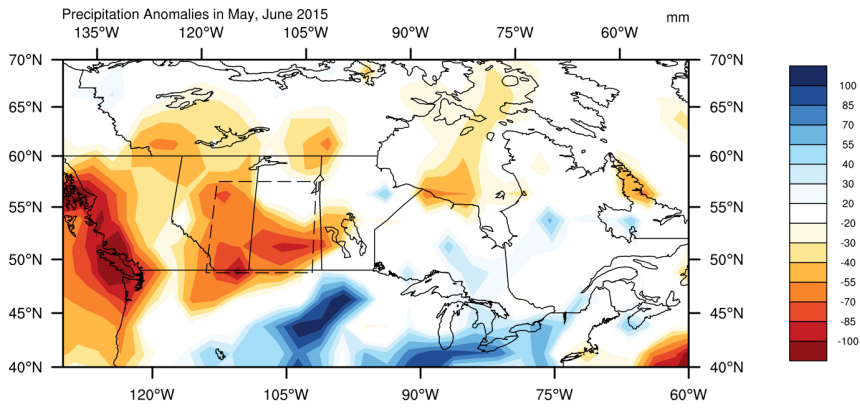
938 Table 1 Correlation between mean precipitation anomaly in the prairie from CMAP and MEI, MJO
939 indices 4. MJO indices and CMAP are from 1979 to 2016.

Deleted: from CMAP

Deleted: CMAP covers 1979 to 2016.

	Correlation	p-value	No. of sample
MEI	-0.096	0.24	156
MJO-4	0.18	0.023	156
MJO-4(NINO4>0)	0.33	0.0015	90
MJO-4(NINO4<0)	-0.01	0.94	66

940



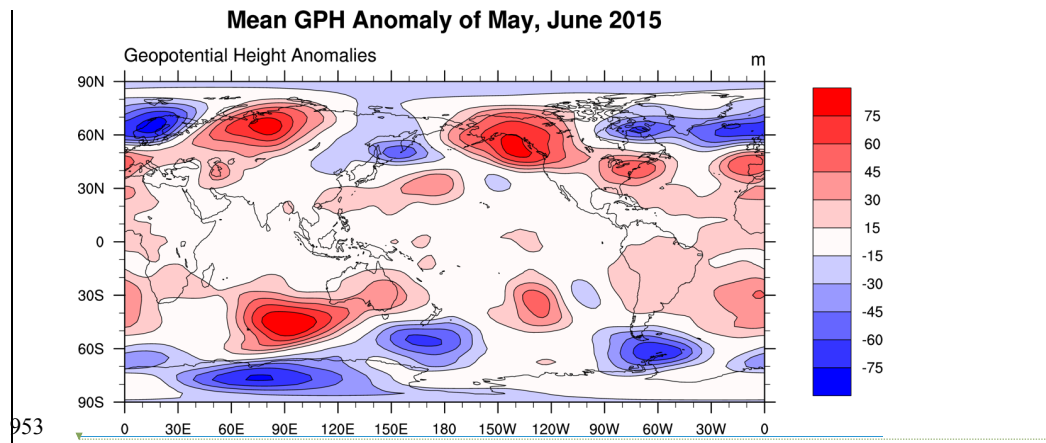
Deleted:

943
944 Fig. 1 Top: Precipitation anomalies (mm) from CMAP over the region (115 W-102.5 W, 50 N-57.5 N)
945 during May and June 2015. Bottom: time series of monthly precipitation anomaly over boxed region
946 between September 2013 and August 2015.

947
948
949

951

952



953

954 Fig. 2 NCEP GPH anomaly at 500hPa during May and June 2015 when the precipitation deficit was the
955 largest.

956

957

958

959

960

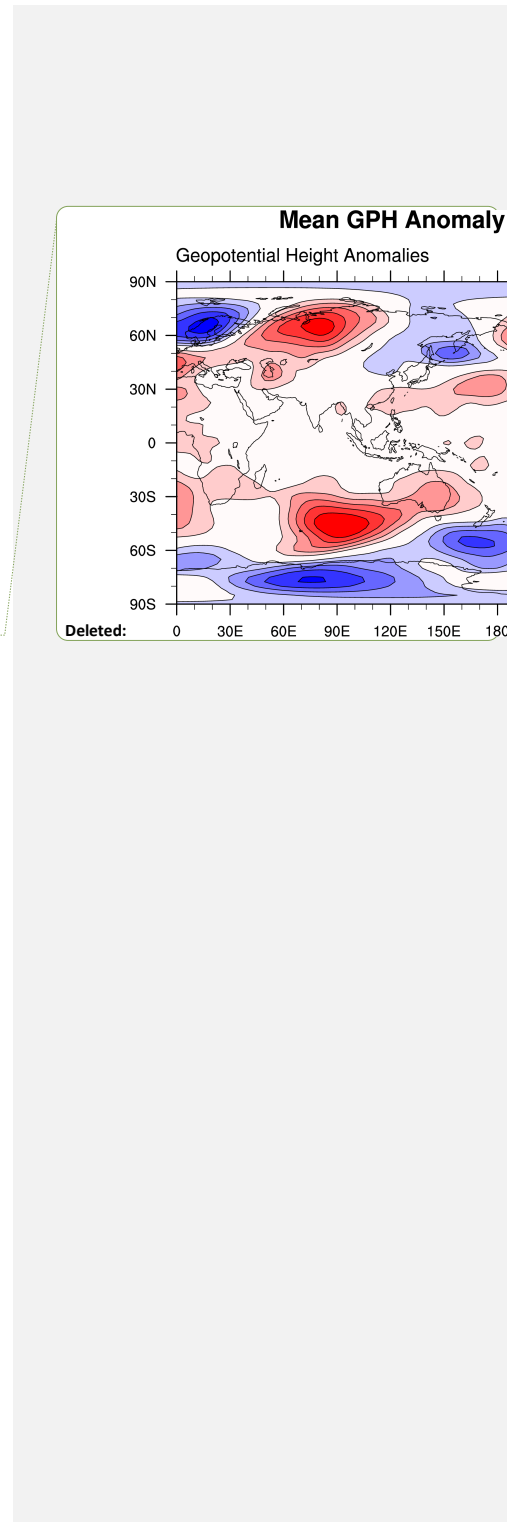
961

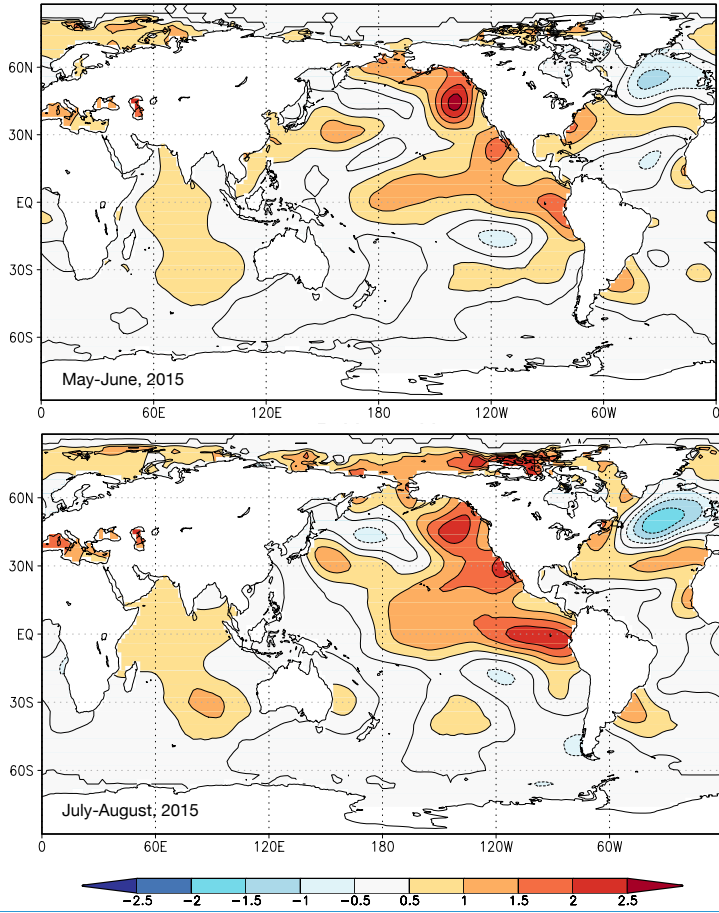
962

963

964

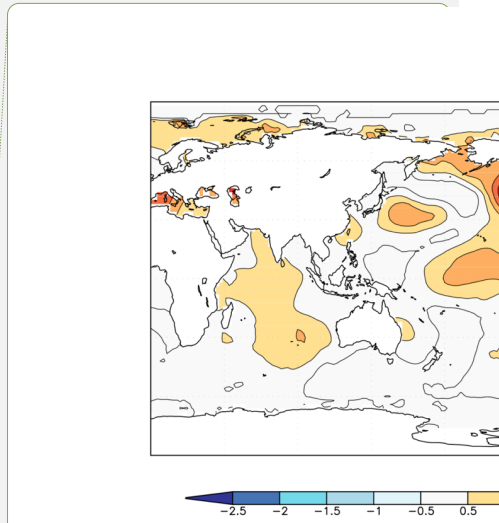
965





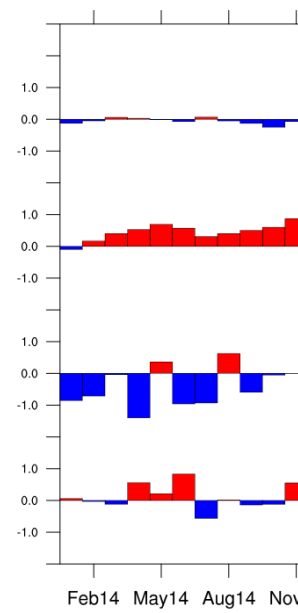
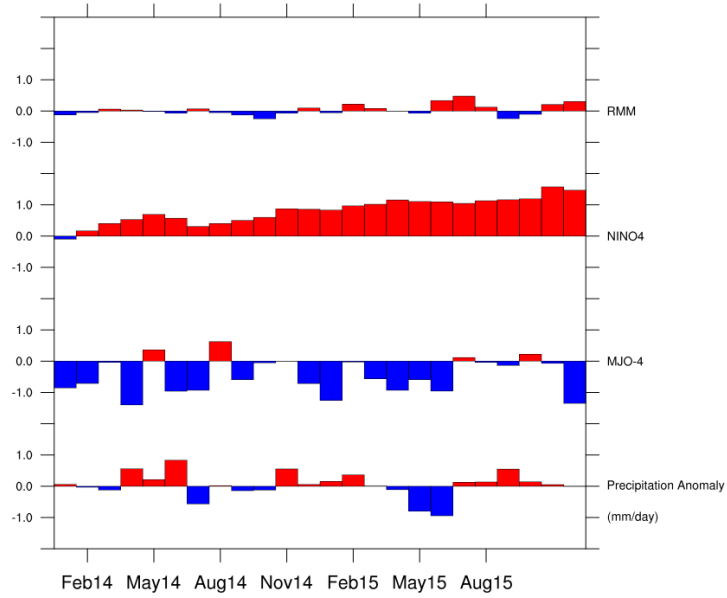
967

968 Fig. 3 The mean SST anomaly (°C) from ERSST v4 for May-June and July-August 2015.



Deleted:

Deleted: in

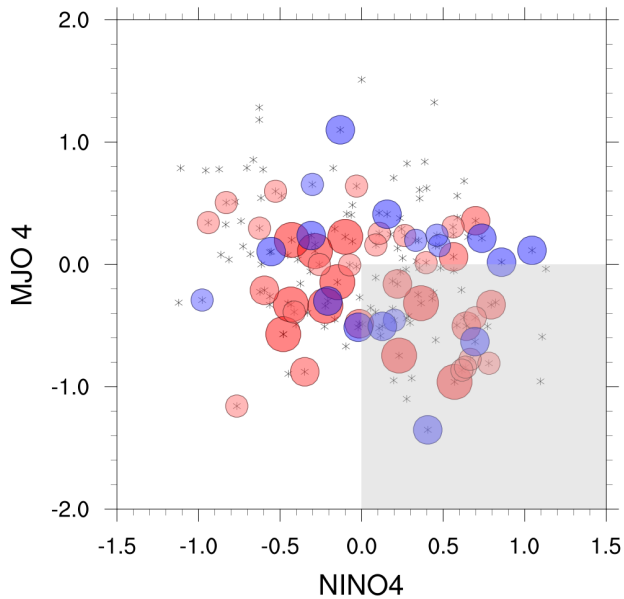


Deleted:

971
 972 Fig. 4 RMM amplitude anomaly, NINO4, MJO 4 indices and precipitation anomaly of Canadian Prairies
 973 from January 2014 to Dec 2015.

974
 975
 976
 977
 978

980



981

982 Fig. 5 The [scatter plot](#) of monthly precipitation anomaly (mm/month) as a function of MJO-4 and
 983 NINO4. Each asterisk represents a month from May to August 1979-2016. Circled asterisk denotes a
 984 month with precipitation anomaly larger than 18 mm/month. The blue circles are months with positive
 985 precipitation anomaly and the red circles are months with negative precipitation anomaly. The sizes of
 986 circles denote the magnitudes of the anomalies (large > 30 mm/month, medium > 24 mm/month,
 987 small > 18 mm/month). The shaded area denotes NINO4 > 0 and MJO-4 index < 0.

988

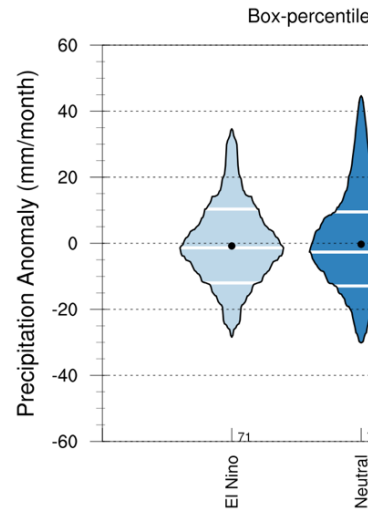
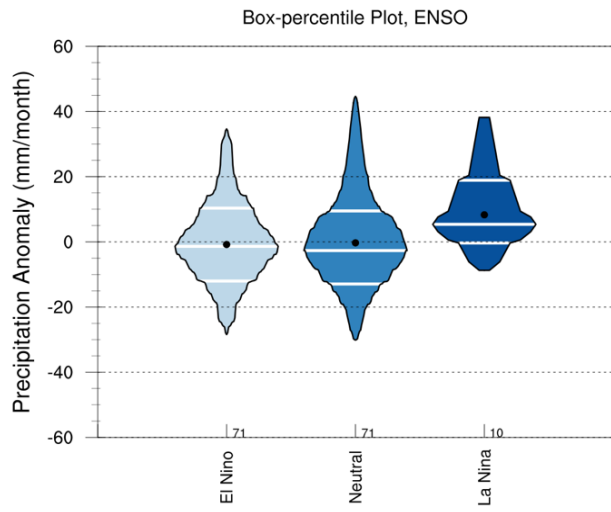
Deleted:

Deleted: scatterplot

Deleted:

Deleted:

Deleted: >



Deleted:

Deleted: for

994

995

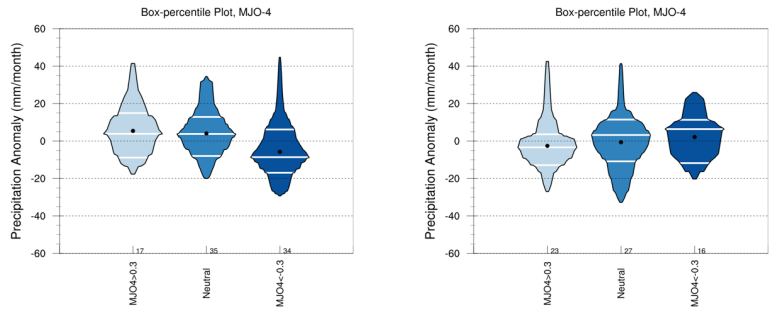
996

997

Fig. 6 The box-percentile plot of Canadian Prairies precipitation anomaly during growing season under different ENSO conditions.

1000

1001



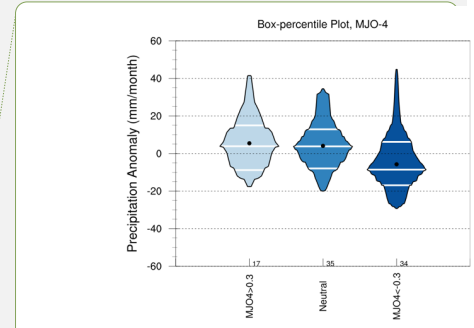
1002

1003

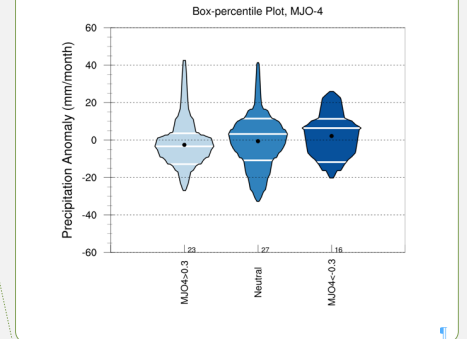
1004

1005

Fig. 7 Box-percentile plots of Canadian Prairies' precipitation anomaly during growing season versus MJO-4 under warm NINO4 (NINO4> 0, left) and cold NINO4 (NINO4<0, right) SST condition.

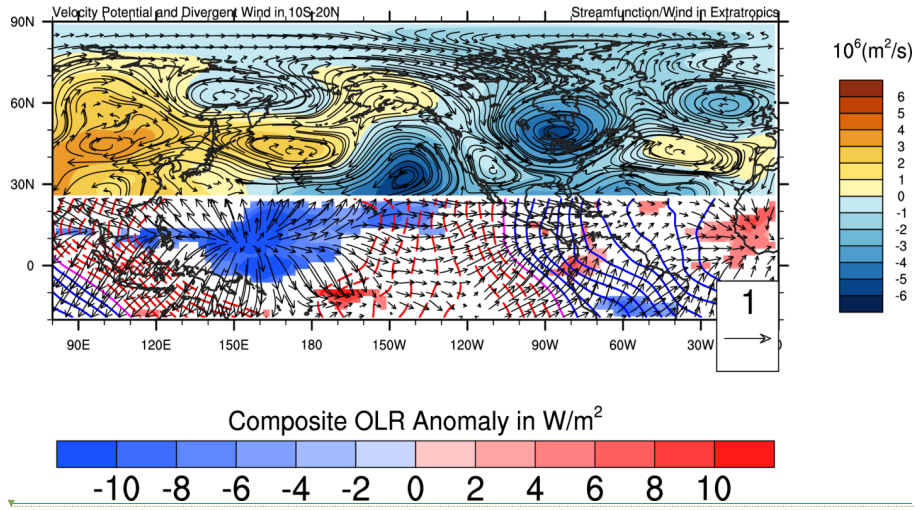


Deleted:



Deleted:

1009



1010

1011

1012 Fig. 8 The regression of stream function, wind field in the extratropics on MJO-4 for May-August with

1013 $NINO4 \geq 0.5$. OLR, velocity potential, and divergent wind in the tropics on MJO-4 indices for May-

1014 August with $NINO4 > 0.5$. The shaded region for the tropical OLR has p-value ≤ 0.05 . Blue shading

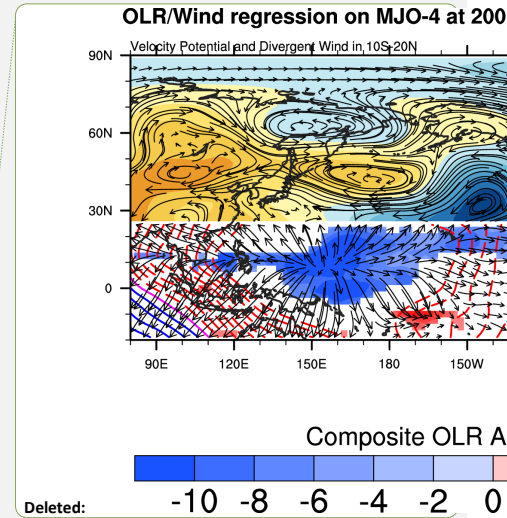
1015 indicates active convection region. Red dashed contour and solid blue contour corresponds to negative

1016 and positive velocity potential, respectively.

1017

1018

1019



Deleted:

Deleted: MEI >

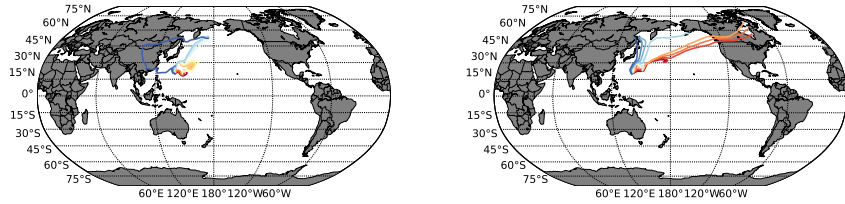
Deleted: Bottom:

Deleted: $NINO4 > 0$.

Deleted: <

Deleted:

Deleted: ↓



1028

1029

1030 *Fig. 9: Ray-tracing result with total wavenumber specified by the mean flow 140-150W and 20-30N for*
 1031 *mean May-August condition with NINO4<-0.5 (left) and NINO4>0.5 (right). Rays originate from 140E,*
 1032 *20N with angles ranging from 0 (red) to 60 degree (dark blue) from zonal direction.*

Summer of 2015 is the first summer after the developing El Nino during 2014-2015 winter. Though the upper-level GPH pattern seen in summer 2015 can be attributed to the SST modes in the Pacific Basin, namely ENSO and NPM, the precipitation in the Western Canadian Prairie is not strongly correlated with either of them. Bonsal and Lawford (1999) found that more extended dry spells tend to occur during the second summer following the mature stage of the El Nino events. The winter precipitation in Canada has been shown to have a strong connection to ENSO (Shabbar et al. 1997), whereas summer precipitations in most regions of western Canada (except the coast of British Columbia and Southern Alberta) do not have significant correlations with ENSO. This is consistent with our investigation using instrumental records from 1948 to 2016.